International Journal of Modern Physics E
© World Scientific Publishing Company

arXiv:1606.08637v1 [nucl-th] 28 Jun 2016

The fusion dynamics for a positive Q-value system: ^{27}Al+^{45}Sc using SEDF and role of spin-orbit interaction potential

Dalip Singh Verma* and Atul Choudhary

Department of Physics and Astronomical Science, Central University of Himachal Pradesh, Dharamshala, District Kangra,(H.P)-176215, INDIA

Received Day Month Year
Revised Day Month Year

The fusion dynamics for a positive Q-value systems: ^{27}Al+^{45}Sc, at near and deep sub-barrier energies has been investigated using the proximity potentials of Skyrme energy density formalism in semi classical extended Thomas Fermi approach for arbitrarily chosen Skyrme forces: SLy4, SIV, SGII and Proximity77 of Blocki and co-workers. The calculated fusion excitation functions for the proximity potentials obtained for Skyrme forces mentioned above and for the Proximity77 have been compared with experimental data. The proximity potential for Skyrme force SIV is found to be the best and is used in the calculations of the quantities like logarithmic derivative, barriers distributions and S-factor. Further, the role of spin-orbit interaction potential in the fusion dynamics of this system has been investigated.

Keywords: Skyrme energy density formalism, spin-orbit interaction potential, logarithmic derivative, barrier distribution and S-factor.

PACS numbers:24.10.-i, 25.60.Pj, 25.70.-z

1. Introduction

During the last decade, the of heavy ion (HI) fusion cross-section measurements has been extended to deep sub-barrier energies and in this energy regime the investigation of fusion excitation functions has revealed new phenomenon like fusion hindrance and enhancement. The signatures of fusion hindrance, the steep fall in fusion excitation function, at deep sub-barrier energies with respect to the standard coupled-channel (CC) calculations was firstly observed by Jiang and co-workers[1] at National Laboratory, Argonne, Illinois (USA) in the year 2002. Since then lot of theoretical and experimental work has been done in this low energy domain, which is of great interest not only in the field of nuclear astrophysics, where fusion hindrance can affect the rate of interstellar reactions like: ^{12}C+^{12}C,[2] but it also incorporate with the synthesis of super-heavy elements.

*dsverma@cuhimachal.ac.in

In a quest to understand this unexpected behavior, Jiang *et al.*[1] measured and calculated the fusion cross-sections using CC calculations and Wong's approximation for the system ^{60}Ni+^{89}Y at deep sub-barrier energies, re-analyzed the same for the systems: ^{58}Ni+^{58}Ni & ^{90}Zr+^{92}Zr and observed fusion hindrance for these systems. These authors proposed that some properties of fused system, like Q-value (not sufficient alone) as a possible cause of fusion hindrance. Later Jiang *et al.*,[3] has shown that the fusion hindrance is a general behavior of positive as well as negative Q-value systems and reproduced the observed behavior of fusion excitation function by incorporating nuclear incompressibility in CC calculations. Similarly, the fusion hindrance is observed[4] for open-shell system: ^{64}Ni+^{64}Ni w.r.t CC calculations and the observed data is reproduced by including nuclear structure inputs. Further, to explain the fusion hindrance, the double folding potential (which was too deep for overlapping nuclei) is supplemented with repulsive core by Misicu and Esbensen[5] along with the effective nucleon-nucleon interaction (v_{NN}), called shallow ion-ion potential. In this context, for looking appropriate potentials, different authors have given different reasons, like Ichikawa *et al.*[6] has suggested two-step model of fusion, where the first step is again determined by CC calculations and second step is determined by using one-dimensional adiabatic potential barrier and accounts well for fusion hindrance observed for the systems: ^{64}Ni+^{64}Ni & ^{58}Ni+^{58}Ni, Ichikawa *et al.*[7] has extended the standard CC calculations by considering smooth transition from sudden to adiabatic states and explained the fusion hindrance for the systems: ^{16}O+^{208}Pb, ^{64}Ni+^{64}Ni & ^{58}Ni+^{58}Ni, Hagino *et al.*[8] fitted the Wood-Saxon potential in CC calculations and concluded that the large diffuseness is required to predict low energy behavior of fusion cross-section and Brink *et al.*[?] suggested that fusion hindrance may be associated with the overlapping of densities of the two colliding nuclei, where the description of the potential failed, even when CC effects are included. Several other reasons for the fusion hindrance has been given in literature.[10–20] In all the calculations discussed above, the experimental behavior is reproduced by modifying nuclear potential in different ways.

So, it is of great interest to see whether the potentials obtained in Skyrme energy density formalism (SEDF) in semi-classical extended Thomas-Fermi approach (see Ref.[21]) and Blocki's proximity potential (Proximity77)[22] are capable of explaining this enigmatic behavior of fusion excitation function or not. As the SEDF has ability to provide different-different nuclear proximity potentials for different Skyrme forces and is expressed as the sum of two different potentials: (i) spin-orbit density dependent (mainly repulsive) and (ii) spin-orbit density independent (mainly attractive). Since spin-orbit interaction potential is mainly repulsive, which is equivalent to the addition of repulsion to the proximity potential, therefore it will be further interesting to see the effects of this interaction potential in the fusion dynamics for the system: ^{27}Al+^{45}Sc, where the fusion cross-section has been measured[23] at deep sub-barrier energies down to about 300 nb, because the standard CC calculations failed to reproduce the observed data for this system. Note that

the SEDF proximity potentials and Proximity77 are used in Wong's approximation for the calculation of fusion cross-section as a function of center of mass energy.

Section 2 describe the methodology for the calculation of interaction potentials, cross-sections, logarithmic derivative, barrier distribution and astrophysical factor. In section 3, calculations and results are discussed and finally section 4 contains the conclusion of the study.

2. Methodology

The following sub-sections give the calculations detail for the Skyrme interaction potential based upon SEDF and Proximity77, fusion cross-section, logarithmic derivative, barrier distribution and finally the astrophysical factor.

2.1. *Skyrme Energy Density Formalism*

The SEDF, defines the nuclear interaction potential as a function of inter-nuclear separation (R) as the difference between the energy expectation value E of the colliding nuclei that are overlapping (at a finite separation distance R) and are completely separated (at $R = \infty$) and is given as,

$$V(R) = E(R) - E(\infty) \tag{1}$$

where $E = \int H(\vec{r})d^3\vec{r}$, is the energy expectation value. The Skyrme Hamiltonian density (see Refs.[21,24]) given as,

$$\begin{aligned} H[\ \rho,\ \tau,\ \vec{J}\ ] = {} & \frac{\hbar^2}{2m}\tau_q + \frac{1}{2}t_0\left[\left(1+\frac{x_0}{2}\right)\rho^2 - \left(x_0+\frac{1}{2}\right)\left(\rho_n^2+\rho_p^2\right)\right] \\ & + \frac{1}{12}t_3\rho^{\alpha_0}\left[\left(1+\frac{x_3}{2}\right)\rho^2 - \left(x_3+\frac{1}{2}\right)\left(\rho_n^2+\rho_p^2\right)\right] \\ & + \frac{1}{4}\left[t_1\left(1+\frac{x_1}{2}\right)+t_2\left(1+\frac{x_2}{2}\right)\right]\rho\tau - \frac{1}{4}\left[t_1\left(x_1+\frac{1}{2}\right)-t_2\left(x_2+\frac{1}{2}\right)\right] \\ & \times\left(\rho_n\tau_n+\rho_p\tau_p\right) + \frac{1}{16}\left[3t_1\left(1+\frac{x_1}{2}\right)-t_2\left(1+\frac{x_2}{2}\right)\right]\left(\vec{\nabla}\rho\right)^2 \\ & - \frac{1}{16}\left[3t_1\left(x_1+\frac{1}{2}\right)+t_2\left(x_2+\frac{1}{2}\right)\right]\left\{\left(\vec{\nabla}\rho_p\right)^2+\left(\vec{\nabla}\rho_n\right)^2\right\} \\ & - \frac{1}{2}W_0\left[\rho\vec{\nabla}.\vec{J}+\rho_n\vec{\nabla}.\vec{J}_n+\rho_p\vec{\nabla}.\vec{J}_p\right] \end{aligned} \tag{2}$$

where $\rho = \rho_p + \rho_n, \tau = \tau_p + \tau_n, \vec{J} = \vec{J}_n + \vec{J}_p$ are nuclear, kinetic, and spin-orbit densities respectively, $x_i, t_i, \alpha_0,$ and W_0 are the Skyrme force parameters, fitted by different authors, (see e.g. Refs.[25,26]) to obtain ground state properties of the nuclei.

The kinetic energy density for nucleon τ_q, upto second order of expansion (enough for numerical convergence[27]), in the semi-classical extended Thomas Fermi

(ETF) approach of SEDF, is

$$\tau_q(\vec{r}) = \frac{3}{5}\left(3\pi^2\right)^{2/3}\rho_q^{5/3} + \frac{1}{36}\frac{(\vec{\nabla}\rho_q)^2}{\rho_q} + \frac{1}{3}\Delta\rho_q + \frac{1}{6}\frac{\vec{\nabla}\rho_q.\vec{\nabla}f_q + \rho_q\Delta f_q}{f_q} - \frac{1}{12}\rho_q\left(\frac{\vec{\nabla}f_q}{f_q}\right)^2 + \frac{1}{2}\rho_q\left(\frac{2m}{\hbar^2}\right)^2\left(W_0\frac{\vec{\nabla}\left(\rho+\rho_q\right)}{2f_q}\right)^2 \quad (3)$$

where $f_q(\vec{r})$ is effective mass form factor, which depend upon the effective mass term (3^{rd} term of Eq. (2)) given as:

$$f_q(\vec{r}) = \frac{m}{m^*(\vec{r})} = 1 + \frac{2m}{\hbar^2}\frac{1}{4}\left\{t_1\left(1+\frac{x_1}{2}\right) + t_2\left(1+\frac{x_2}{2}\right)\right\} - \frac{2m}{\hbar^2}\frac{1}{4}\left\{t_1\left(x_1+\frac{1}{2}\right) - t_2\left(x_2+\frac{1}{2}\right)\right\}\rho_q(\vec{r}) \quad (4)$$

where $q = n$ *or* p for neutron or proton, and $m^*(\vec{r})$ is effective mass.

The spin $\vec{J}$ being purely a quantal property has no contribution to the semi-classical functional in the lowest order, the second order-contribution is,

$$\vec{J}_q(\vec{r}) = -\frac{2m}{\hbar^2}\left(\frac{1}{2}W_0\right)\frac{1}{f_q}\rho_q\vec{\nabla}(\rho+\rho_q) \quad (5)$$

The nuclear interaction potential is calculated in slab approximation, for details see Refs.,[21,28] given as,

$$V_N(R) = 2\pi\bar{R}\int_{s_0}^{\infty} e(s)ds, \quad (6)$$

where $\bar{R} = R_{01}R_{02}/(R_{01}+R_{02})$ is the mean curvature radius, R_{0i} are the central radii of interacting nuclei and $e(s)$ is the interaction energy per unit area between two flat slabs of semi-infinite nuclear matter with surfaces parallel to the $x-y$ plane and moving in the z-direction separated by distance s, having a minimum value s_0, is given by,

$$\int_{s_0}^{\infty} e(s)ds = \int\left[H(\rho,\tau,\vec{J}) - \{H_1(\rho_1,\tau_1,\vec{J}_1) + H_2(\rho_2,\tau_2,\vec{J}_2)\}\right]dz. \quad (7)$$

As τ and $\vec{J}$, both are function of ρ, so $H[\rho,\tau,\vec{J}]$ becomes function of ρ only. Since both spin-orbit density dependent part (repulsive) and independent part (attractive) behaves differently, so Eq. (6) can be written as,

$$V_N(R) = V_P(R) + V_J(R) \quad (8)$$

The nuclear density, $\rho_i = \rho_{n_i} + \rho_{p_i}$, where $\rho_{n_i} = (N_i/A_i)\rho_i$ and $\rho_{p_i} = (Z_i/A_i)\rho_i$, $i = 1,\ 2$ for two colliding nuclei,[21] is the two parameter TF density and in slab approximation with temperature dependence included becomes,

$$\rho_i(z_i,T) = \rho_{0i}(T)\left[1+\exp\left(\frac{z_i - R_{0i}(T)}{a_{0i}(T)}\right)\right]^{-1} \quad (9)$$

with $-\infty \leq z \leq \infty$ *and* $z_2 = R - z_1$, and central density is,

$$\rho_{0i}(T) = \frac{3A_i}{4\pi R_{0i}^3(T)} \left[1 + \frac{\pi^2 a_{0i}^2(T)}{R_{0i}^2(T)}\right]^{-1} \tag{10}$$

The central radii $R_{0i}(T = 0)$, surface thicknesses $a_{i0}(T = 0)$ and temperature dependence of these parameters are taken, from Ref.[21] The Proximity77 is tried here as an alternate to the SEDF proximity potential, is given as:

$$V_N = 4\pi \bar{R}\gamma b\Phi(s) \tag{11}$$

where $\gamma = 0.9517[1 - 1.7826\{(N - Z)/A\}^2]$ MeV fm^{-2} is nuclear surface energy coefficient, $b = 0.99$ fm is nuclear surface width and Φ is the universal function, which depends upon the separation 's' between the surfaces of interacting nuclei and is given as,

$$\Phi(s) = \begin{cases} -\frac{1}{2}(s - s_0)^2 - 0.0852(s - s_0)^3; & s \leq 1.2511 \\ -3.437 \exp\left(-\frac{s_0}{0.75}\right); & s \geq 1.2511 \end{cases}$$

where $s_0 = 2.54$ is the minimum separation between two flat slabs. The Coulomb contribution, $V_C(R) = kZ_1Z_2/R$ is added directly to Eq. (8) or Eq. (11) to obtain the total interaction potential $V_T(R)$, where $k = 1.44$ MeV fm.

To calculate the fusion cross-section as a function of centre of mass-energy (E_{cm}), the barrier height (V_B), barrier position (R_B) and barrier curvature ($\hbar\omega_0$) of total interaction potential are used in Wong's formula,[29] is given as

$$\sigma(E_{cm}) = \frac{\hbar\omega_0 R_B^2}{2E_{cm}} \ln\left[1 + \exp\left\{\frac{2\pi}{\hbar\omega_0}(E_{cm} - V_B)\right\}\right] \tag{12}$$

where $\hbar\omega_0$ is obtained in parabolic or inverted harmonic approximation. Further to amplify the fusion cross-section at deep sub-barrier energies and near barrier energies the logarithmic derivative of energy weighted cross-section and barrier distribution has been calculated respectively. The logarithmic derivative introduced by Jiang *et al.*[1] is given as,

$$L(E_{cm}) = d\left[\ln(E_{cm}\sigma)\right]/dE_{cm} = \frac{1}{\sigma E_{cm}} \frac{d(E_{cm}\sigma)}{dE_{cm}}. \tag{13}$$

The barrier distribution of energy weighted cross-section is,[30]

$$B(E_{cm}) = \frac{d^2(E_{cm}\sigma)}{dE_{cm}^2} \tag{14}$$

An alternative representation of fusion cross-section, frequently used in nuclear astrophysics to predict low energy behavior of nuclear reactions, is astrophysical factor[31] given as

$$S(E_{cm}) = E_{cm}\sigma \exp\{2\pi(\eta - \eta_0)\} \tag{15}$$

where $\eta(= 0.1575Z_1Z_2\sqrt{\mu/E_{cm}})$ is the Sommerfield parameter, Z_1, Z_2 are the charges of interacting nuclei and $\mu(= A_1A_2/(A_1 + A_2))$ is the reduced mass. The parameter η_0 is calculated at Coulomb energy ($E_c = Z_1Z_2e^2/(R_1 + R_2)$). The strong

energy dependence of fusion excitation function depends upon Coulomb barrier, and the S-factor remove this dependence by eradicating the Coulomb component.

3. Calculations and Results

First, we have calculated the fusion excitation functions for a positive Q-value (Q = 9.63 MeV) system: ^{27}Al+^{45}Sc, using two types of potentials. One obtained within the semi-classical extended Thomas-Fermi approach of SEDF for arbitrarily chosen Skyrme forces SLy4, SIV, SGII and other obtained from the proximity pocket formula (Proximity77). The potential characteristics:- barrier position (R_B), barrier

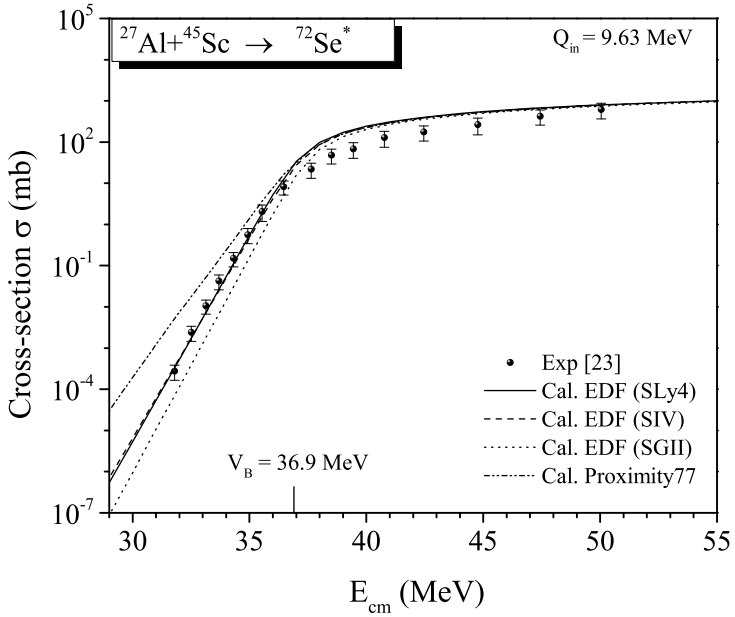

Fig. 1. A comparison of the calculated fusion excitation functions with the proximity potential for arbitrarily chosen Skyrme forces: SLy4, SIV and SGII and for the fusion excitation function obtained using Proximity77 with experimental data[23] as a function of E_{cm}.

height (V_B) and barrier curvature ($\hbar\omega_0$) of the two types of the potentials are used in Wong's formula, Eq. (12), to obtain the fusion cross-section as a function of E_{cm} (i.e. the fusion excitation function). Out of SEDF proximity potentials for SLy4, SIV, SGII and Proximity77 used in the fusion excitation function calculations, the proximity potential for Skyrme force SIV has been found to be the best (see Fig. 1) and hence is chosen for rest of the calculations. Next, the role of spin-orbit interaction potential in the fusion dynamics of the system i.e. in the calculations of the fusion cross-section, logarithmic derivative, barrier distribution and S-factor has been investigated.

Figure 1, shows the comparison of the calculated fusion excitation functions for the proximity potentials obtained for Skyrme forces SLy4 (solid line), SIV (dashed line) and SGII (dotted line) with the experimental data[23] (solid spheres with error bars). The dash dot-dot line represent the fusion excitation function obtained using Proximity77. It is found from the comparison of the calculated fusion excitation functions, shown in Fig. 1, with the observed data[23] that for below barrier energies the cross-section is best reproduced by the proximity potential for two forces: SLy4 and SIV. The excitation functions with the potentials obtained for Skyrme forces SGII and for the Proximity77 are under-estimating and over-estimating with respect to the experimental data, respectively. Above barrier energies all the potentials are showing almost equivalent results but among the potentials for SLy4 and SIV Skyrme forces, SIV is closer to the experimental data and is chosen for rest of the calculations. As in Ref.[32] repulsion/repulsive potential is added to the proximity potential to reproduce the observed data. In SEDF, the nuclear interaction potential

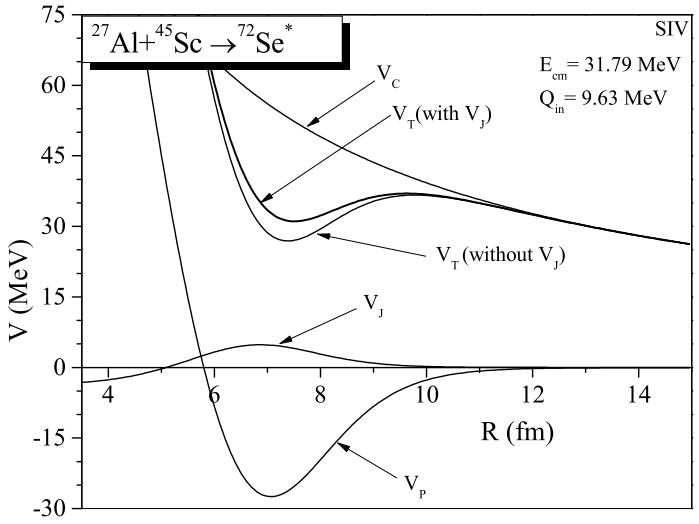

Fig. 2. The nuclear proximity potential V_P, spin-orbit interaction potential V_J, Coulomb interaction potential V_C and the total interaction potential V_T with and without spin-orbit interaction potential as a function of inter-nuclear separation R for the Skyrme force SIV.

has a repulsive part (spin-orbit density dependent part) in addition to the attractive part (spin-orbit density independent term) and hence the effect of latter part of interaction potential on fusion dynamics of ^{27}Al+^{45}Sc has been studied for the first time and is discussed below.

Figure 2 shows different contributing potentials: V_P, V_J and V_C to the total interaction potential V_T (with and without V_J) as a function of inter-nuclear dis-

tance (R). It is clear from the Fig. 2 that the addition of spin-orbit interaction potential leads to the following minor changes: (i) shift of potential barrier to the lower position (i.e. R_B changes from 9.801 fm to 9.671 fm) and (ii) V_B changes from 36.661 MeV to 36.987 MeV (iii) $\hbar\omega_0$ from 2.91 MeV to 2.71 MeV. The corre-

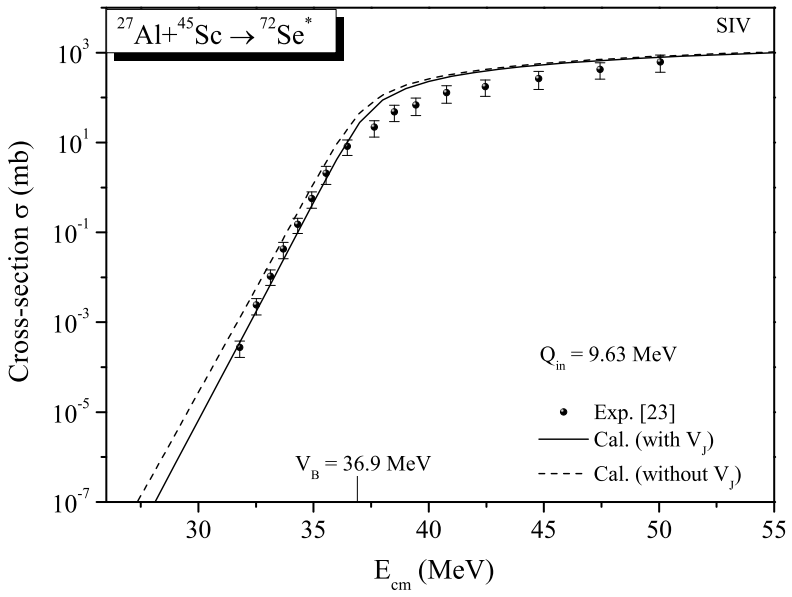

Fig. 3. A comparison of the calculated fusion excitation function with and without spin-orbit interaction potential in proximity potential for Skyrme force SIV with experimental data,[23] as a function of E_{cm}.

sponding changes in fusion excitation function is shown in Fig. 3, where the fusion excitation function without V_J contribution in total interaction potential (dashed line) changes to the fusion excitation function (solid line) when V_J contribution is included. It is clear from the Fig. 3, that the total interaction potential with spin-orbit interaction potential is reproducing data nicely. This means in Skyrme energy density formalism, the addition of spin-orbit interaction potential that is the repulsive part to the proximity part of the nuclear potential enable it to reproduce the experimental data below the barrier very well. Similar calculations are presented in Ref.[23] using shallow potential model developed to study the fusion hindrance in negative Q-value systems, where repulsion is added to the interaction potential to reproduces the experimental data.

In Fig. 4, the logarithmic derivative of energy weighted fusion cross-section have been shown, the solid line shows the logarithmic derivative derived from the fusion excitation function calculated using the total interaction potential including the

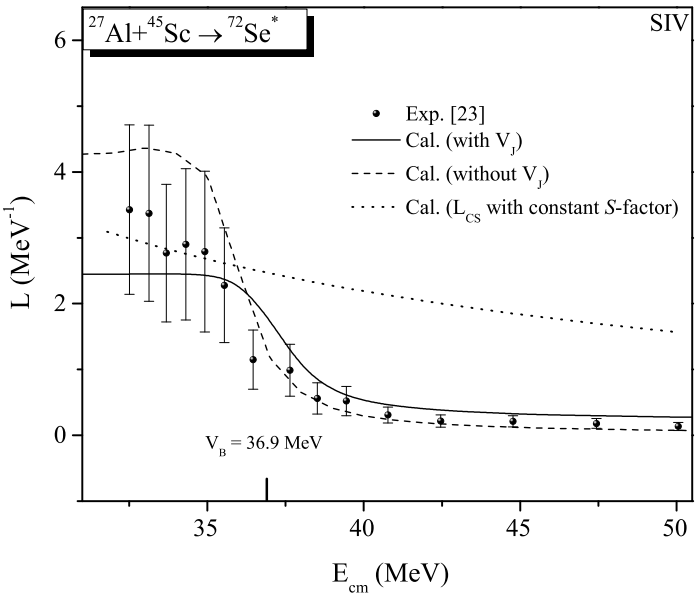

Fig. 4. The calculated logarithmic derivative of energy weighted fusion cross-section with and without spin-orbit interaction potential in proximity potential for Skyrme force SIV and is compared with the experimental data[23] as a function of E_{cm}.

spin-orbit interaction term, while the dashed line is for the same but calculated by excluding spin-orbit interaction potential. Both these curves develop rapidly with decrease in center of mass energy near the interaction barrier energies and saturate further with the decrease in E_{cm}-value, showing that L is independent of E_{cm}. The dotted line is for the logarithmic derivative corresponding to constant S-factor, given as $L_{CS} = \pi\eta/E_{cm}$, the value corresponding to E_{cm} where S-factor develops maxima. In other words S-factor may observe maxima where L_{CS} intersect with experimental L. The interaction potentials with and without spin-orbit interaction potential are reproducing the data with in limits of errors.

Figure 5 shows a comparison of the calculated barrier distribution, which is a magnified view of fusion cross-sections at energies near the interaction barrier, with the experimental data[23] (shown by solid spheres with error bars) as a function of E_{cm}. The solid line shows the barrier distribution when V_J term included in the total interaction potential while the dashed line is for the same but when V_J term is excluded. Our calculations with V_J term is reproducing the data nicely near and below barrier energies and is showing an oscillating behavior for above barrier energies, the oscillations are stronger for the case when total interaction potential exclude V_J term. Note that the interaction barrier height $V_B = 36.9$ MeV is for the interaction potential including spin-orbit term.

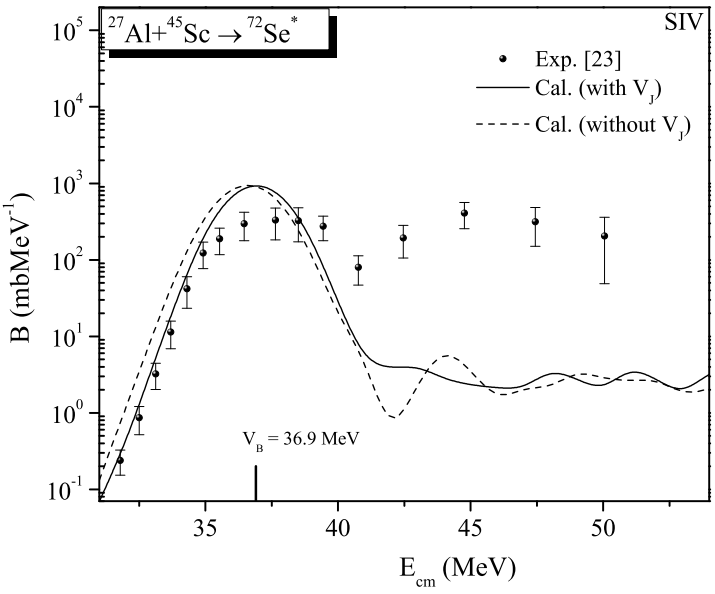

Fig. 5. The barrier distribution calculated with and without spin-orbit interaction potential in the proximity potential for Skyrme force SIV is compared with the experimental data[23] as a function of E_{cm}.

Alternate representation to the fusion cross-section is S-factor and is required due to the fact that the fusion cross-section varies by many order of magnitude below the interaction barrier, here for this system ^{27}Al + ^{45}Sc it is 6 orders, and at the same time it removes the dominating influence of the Coulomb barrier transmission factor that inhibits the broad resonance structure in fusion excitation function.[33] Figure 6 shows comparison of the calculated S-factor with experimental data[23] (solid spheres) where solid line is for the case when V_J is included in the total interaction potential and dashed line when V_J is excluded. For energies above barrier both cases gives same results while below barrier energies the interaction potential including the spin-orbit term is nicely reproducing the experimental results. The S-factor increases rapidly with decrease in center of mass energy and almost saturate near the barrier energies and then again increases rapidly with further decrease in E_{cm}. The broad maxima near deep sub barrier energies may be an indication for the resonance structure in the excitation function but the confirmation demands the experimental data to be available that lower E_{cm}. Our calculations shows rapid increase in S-factor after getting saturation region and hence is not in favor of resonance structure in the fusion excitation function for this system.

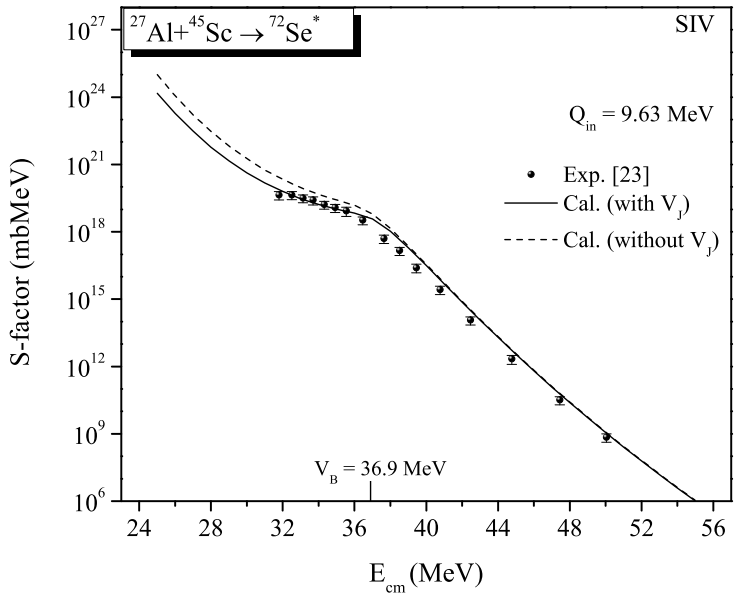

Fig. 6. The S-factor calculated with and without spin-orbit interaction potential in the proximity potential for Skyrme force SIV and is compared with experimental data.[23]

4. Conclusion

We conclude that the interaction potential obtained in SEDF for Skyrme force SIV is found to be the better than potentials obtained for SLy4, SGII and the Proximity77 potential for the fusion dynamics of $^{27}Al + ^{45}Sc$ system. The inclusion of spin-orbit interaction potential in the proximity potential, which is equivalent to the addition of repulsion to the nuclear potential, reproduces the observed data better than when it is excluded. The calculated barrier distribution gives comparatively stronger oscillations for interaction potential excluding spin-orbit term for energies above barrier. The clear maxima in S-factor is not found, for deep sub-barrier energies, in our calculations as well as in the experimental data which indicates the absence of structure in fusion excitation function. Our calculations shows the strong energy dependence of astrophysical factor for far below the barrier energies and hence more experimental data is required at these energies to see the behavior of fusion excitation functions for this system.

References

1. C. L. Jiang, H. Esbensen, *et al.,* Phys. Rev. Lett **89**, 052701 (2002).
2. L. R. Gasques, *et al.,* Phys. Rev. C **76**, 035802 (2007).
3. C. L. Jiang, B . B. Back, *et al.,* Phys. Lett. B **640**, 18 (2006).
4. C. L. Jiang, K. E. Rehm, *et al.,* Phys. Rev. Lett **93**, 012701 (2004).

5. S. Misicu, H. Esbensen, Phys. Rev. C **75**, 034606 (2007).
6. T. Ichikawa, K. Hagino, *et al.,* Phys. Rev. C **75**, 057603 (2007).
7. T. Ichikawa, K. Hagino, *et al.,* Phys. Rev. Lett **103**, 202701 (2009).
8. K. Hagino, N. Rowley, *et al.,* Phys. Rev. C **67**, 054603 (2003).
9. D. M. Brink, Prog. Theor. Phys. Suppl **154**, 268 (2004).
10. V. S. Ramamurthy, A. K. Mohanty, *et al.,* Phys. Rev. C **41**, 2702 (1990).
11. C. J. Lin, Phys. Rev. Lett **91**, 229201 (2003).
12. B. G. Giraud, S. Karataglidis, *et al.,* Phys. Rev. C **69**, 064613 (2004).
13. W. M. Seif, J. Phys. G **30**, 1231 (2004).
14. S. V. S. Sastry, S. Kailas, *et al.,* Pramana J. Phys. **64**, 47 (2005).
15. L. C. Chamon, M. S. Hussein, *et al.,* Braz. J. Phys. **37**, 1177 (2007).
16. A. S. Umar, V. E. Oberacker, Phys. Rev. C **77**, 064605 (2008).
17. V. V. Sargsyan, G. G. Adamian, *et al.,* Eur. Phys. J. A**45**, 125 (2010).
18. V. M. Shilov, Phys. At. Nucl, **75**, 449 (2012).
19. R. A. Kuzyakin, V. V. Sargsyan, *et al.,* Phys. At. Nucl, **75**, 439 (2012).
20. C. L. Jiang, B. B. Back, *et al.,* Phys. Rev. Lett **110**, 072701 (2013).
21. R. K. Gupta, Dalip Singh, *et al.,* J. Phy. G: Nucl. Part. Phys **36**, 075104 (2009).
22. J. Blocki, J. Randrup, *et al.,* Ann. Phys. NY **105**, 427 (1977).
23. C. L. Jiang, K. E. Rehm, *et al.,* Phys. Rev. C **81**, 024611 (2010).
24. D. Vautherin, D. M. Brink, Phys. Rev. C **5**, 626 (1972).
25. M. Brack, C. Guet, *et al.,* Phys. Rep. **123**, 275 (1985).
26. J. Friedrich and P. G. Reinhardt, Phys. Rev. C **33**, 335 (1986).
27. J. Bartel and K. Bencheikh, Eur. Phys. J. A **14**, 179 (2002).
28. R. K. Gupta, Dalip Singh and W. Greiner, Phys. Rev. C **75**, 024602 (2007).
29. C. Y. Wong, Phys. Rev. Lett. **31**, 766 (1973).
30. N. Rowley, G. R. Satchler, *et al.,* Phys. Lett. B **254**, 25 (1991).
31. E. M. Burbidge, G. Burbidge, *et al.,* Rev. Mod. Phys. **29**, 547 (1957).
32. G. Montagnoli, A. M. Stefanini, *et al.,* Phys. Rev. C **85**, 024607 (2012).
33. K. A. Erb and D. A. Bromley, in *Treastise in Heavy -ion Science,* Vol. 3, ed. D. A. Bromley (Plenum, 1985).